04 Jul 2022

Combination of High PH and an Antioxidant Improves Chemical Stability of Two-Dimensional Transition-Metal Carbides and Carbonitrides (MXenes) in Aqueous Colloidal Solutions

Shuohan Huang

Vadym Mochalin
Missouri University of Science and Technology, mochalinv@mst.edu

Recommended Citation

S. Huang and V. Mochalin, "Combination of High PH and an Antioxidant Improves Chemical Stability of Two-Dimensional Transition-Metal Carbides and Carbonitrides (MXenes) in Aqueous Colloidal Solutions," *Inorganic Chemistry*, vol. 61, no. 26, pp. 9877 - 9887, American Chemical Society, Jul 2022.
The definitive version is available at https://doi.org/10.1021/acs.inorgchem.2c00537

Inorganic Chemistry

pubs.acs.org/IC

Article

Combination of High pH and an Antioxidant Improves Chemical Stability of Two-Dimensional Transition-Metal Carbides and Carbonitrides (MXenes) in Aqueous Colloidal Solutions

Shuohan Huang and Vadym N. Mochalin*

Cite This: *Inorg. Chem.* 2022, 61, 9877−9887

Read Online

ACCESS | Metrics & More | Article Recommendations | Supporting Information

ABSTRACT: MXenes, a large family of two-dimensional (2D) transition-metal carbides/nitrides, have attracted increased attention in recent years because of their excellent electronic, mechanical, thermal, and optical properties. Studying chemical properties of MXenes is important to prolong the shelf life of their colloids and provide robust performance of MXenes in devices and applications. While the role of MXene reactivity with the environment, including water and components of air, is becoming more recognized, less is known about the role of parameters influencing the reactivity. In this work, we investigate the individual and combined effects of the pH and antioxidant on chemical stability of Ti_2CT_x, Ti_3CNT_x, and $Ti_3C_2T_x$ MXenes using GC, XPS, UV−vis, and Raman spectroscopy. In contrast to indirect indicators of MXene degradation, such as film conductivity or performance in electrochemical energy storage systems, we focus on detection of reaction products as the most sensitive and direct way of monitoring the chemical transformations of MXenes. Based on our knowledge of MXene chemistry and interactions with the environment, we propose a combination of sodium hydroxide and sodium L-ascorbate to effectively slow down degradation of MXenes in colloidal solutions by suppressing their hydrolysis and oxidation reactions, respectively.

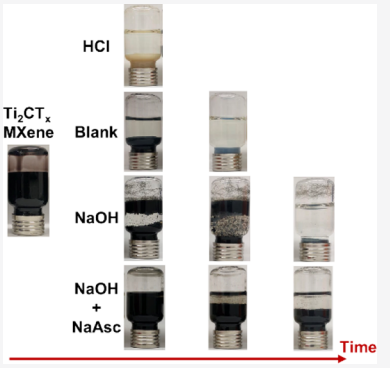

INTRODUCTION

Over the past 10 years, MXenes have been increasingly researched in a broad range of applications[1−4] due to their excellent electronic, mechanical, thermal, and optical properties.[5−8] These 2D forms of transition-metal carbides/nitrides with a general formula $M_{n+1}X_nT_x$ (n = 1−4),[9,10] where M represents an early transition metal, X is carbon and/or nitrogen, and T is the terminating functional groups (-F, -O-, -OH, -Cl, *etc.*), are most commonly synthesized by wet chemical etching from their precursor MAX phases, where A is a group 13 or 14 element.[11] Upon synthesis, MXenes are dispersed in a colloidal state in aqueous media, which is also a preferred way to store them because of the hydrophilic nature of these materials and advantages of using water as the solvent. The unique combination of hydrophilicity and high electrical conductivity ("conductive clays"[6]) and ability to accommodate intercalants[12] are beneficial for various applications of MXenes, such as energy generation and storage,[13−16] electromagnetic interference shielding,[1,17] water purification,[18,19] sensing,[20−22] *etc.* However, MXenes are unstable in aqueous colloids. For example, titanium carbide MXenes spontaneously degrade into TiO_2 and CH_4 over time at room temperature,[23,24] in striking contrast to their bulk counterparts, *e.g.*, bulk titanium carbide, which is chemically stable in these conditions,[25,26] although the very surface of bulk TiC (10−15 nm) can also be hydrolyzed.[27]

Little is known about the chemical reactivity of 2D forms of transition-metal carbides/nitrides and even less about the role of factors, such as temperature, solution concentration, MAX phase precursor, pH, *etc.*, which may affect the reactivity. In view of the importance of the problem, over the past few years attempts have been made to suppress MXene degradation by different researchers. Nicolosi *et al.* proposed refrigeration and a de-aerated environment to substantially improve the shelf life of $Ti_3C_2T_x$ and Ti_2CT_x MXenes in aqueous colloids.[28] Low temperature slows down many exothermic reactions, and freezing MXene solutions to below −20 °C is an efficient way to prolong their shelf life.[29,30] However, the processes of MXene hydrolysis, although slowed down, never completely stop at these temperatures. Radovic *et al.* have demonstrated that sodium L-ascorbate, a known antioxidant, can effectively protect Ti_3C_2 MXene from oxidation.[31] Hypothesizing that degradation of MXenes starts from the edges and defects of the flakes,[28,32] Barsoum *et al.* have proposed to cap supposedly positively charged edges of MXene flakes with polyphosphates

Received: February 16, 2022
Published: June 17, 2022

https://doi.org/10.1021/acs.inorgchem.2c00537
Inorg. Chem. 2022, 61, 9877−9887

and experimentally demonstrated that indeed, the degradation of Ti_3C_2 and V_2C MXenes in aqueous colloids is suppressed upon addition of sodium polyphosphate ("capping agent").[33] The quality and synthesis procedure of the MAX phase precursor can also affect chemical stability of the corresponding MXene. Gogotsi *et al.* have shown that Ti_3C_2 MXene is less stable when the precursor, Ti_3AlC_2, is synthesized using titanium carbide as the carbon source, whereas the MAX phase synthesized using graphite as the carbon source yields a more chemically stable MXene.[34] Later, they demonstrated a modified synthesis method (changing the composition of TiC:Ti:Al = 2:1:1 from a molar ratio to a mass ratio) that produced a less defective MAX phase due to an excess of Al, yielding in turn a less defective MXene that, according to the authors, can be stored for years in an ambient environment.[35] However, no analysis of gaseous decomposition products has been attempted in their study.

In our own prior work, hydrolysis was shown to be one of the main reactions leading to MXene degradation in aqueous colloids.[23,24] Just preventing oxidation is not enough to avoid degradation of MXenes in aqueous media. The rate of hydrolysis processes may significantly depend on the pH of the environment. However, only a handful of results on this topic are available in the literature: on the one hand, accelerated MXene degradation in basic media was reported and explained due to the reaction between MXene and OH^-;[36] on the contrary, Koo *et al.* reported that MXene dispersions are more prone to degradation in an acidic environment, which the authors explained to be due to protonation of the neutral -OH groups attached on the MXene surface, leading to a stronger electron localization on Ti atoms.[37]

In our opinion, these and other contradictory results related to MXene chemical stability in the colloidal state require further investigation and are at least partly due to the indirect measurements of MXene reactivity, where conclusions are made based on the data of MXene thin film conductivity or performance of MXene electrodes in electrochemical energy storage devices, or by analysis of solid decomposition products. In particular, special care needs to be exercised when an indirect measure of MXene stability (such as electrical conductivity or electrochemical performance) may be not sensitive enough to the real extent of chemical reactions leading to material degradation. In this regard, direct registration of the products of MXene reactions provides a clearer and better way to study reactivity of these materials. Analysis of carbon containing gaseous decomposition products, such as methane, is particularly well suited to monitor the kinetics of a carbide MXene degradation[24] because (i) CH_4 and similar molecules can only be released when all bonds between the carbon atom and its surrounding M atoms in MXene are completely broken, which is an unmistakable indication of MXene structure degradation; (ii) CH_4 can be detected in the gaseous phase with high accuracy and unmatched sensitivity using standard analytical chemistry techniques such as gas chromatography and vibrational spectroscopy; (iii) analysis of evolved gas can be performed without complications typical for the analysis of solids, *e.g.*, interference of Raman patterns of MXenes and the corresponding metal oxides or the need to manually deconvolute XPS peaks corresponding to different oxidation states of transition metals in MXenes and their corresponding partially or fully formed M oxides, *etc.* Of course, many other techniques can be used complementary to gas analysis to yield further insights into the mechanisms of reactions involving MXenes.

In this work, we investigate the chemical stability of Ti_2CT_x, Ti_3CNT_x, and $Ti_3C_2T_x$ MXenes over time in aqueous colloidal solutions at different initial pH values ranging from 2 to 11 by direct analysis of the gaseous reaction products using gas chromatography (GC) and Raman spectroscopy, complemented by monitoring MXene concentration in solution with UV−vis spectroscopy, as well as measurements of electrical conductivity of MXene films and post-mortem analysis of solid products of MXene degradation with X-ray diffraction (XRD), Raman, and X-ray photoelectron spectroscopy (XPS). Using a pH-inert electrolyte (NaCl), we attempted to compensate for the effects of the counterions introduced to the solution that may interfere with the effects of pH when a base or acid is used. Finally, we propose a synergistic way to suppress MXene degradation and prolong their shelf life by effectively inhibiting both, oxidation and hydrolysis. We believe that our results will provide further guidelines for developing improved storage strategies for MXene aqueous colloidal solutions and will contribute to further understanding of fundamental chemical properties of 2D transition-metal carbides and carbonitrides.

EXPERIMENTAL SECTION

Synthesis of MAX Phases. MAX phases Ti_2AlC, Ti_3AlCN, and Ti_3AlC_2 were synthesized by known techniques.[24] To synthesize Ti_2AlC, TiC (99.5%, Alfa Aesar), Ti (99.5%, Alfa Aesar), and Al (99.5%, Alfa Aesar) powders were mixed in a 0.85:1.15:1.05 molar ratio for 12 h in a polyethylene jar with glass beads. The mixture was heated using an alumina tube furnace (GSL-1800x, MTI Corporation) at 10 °C/min to 1400 °C and held at this temperature for 4 h under Ar flow. Ti_3AlC_2 was synthesized by mixing Ti, Al, and graphite (99%, Alfa Aesar) powders in a 3:1.1:1.88 molar ratio for 12 h in a polyethylene jar aided by glass beads. The mixture was heated at 10 °C/min to 1550 °C and held at this temperature for 2 h under Ar flow. Ti_3AlCN was synthesized by mixing Ti, AlN (98%, Sigma-Aldrich), and graphite powders in a 3:1:1 molar ratio for 12 h in a polyethylene jar with glass beads. The mixture was heated at 10 °C/min to 1500 °C and held at this temperature for 2 h under Ar flow. MAX phase powders were obtained by drilling holes in the sintered ceramic samples, producing filings, which were collected and sieved through a 325 mesh (45 μm) sieve. The XRD patterns in Figure S1 confirm successful synthesis of MAX phases. However, because of a small amount of impurities detected in the as-synthesized Ti_3AlCN, commercial Ti_3AlCN powder was also purchased (XRD pattern is shown in Figure S2), and degradation kinetics experiments were repeated with the commercial MAX-phase derived MXene. No significant differences in chemical behavior of Ti_3CN MXenes derived from commercial and in-house MAX phases were observed.

Synthesis of MXenes. Ti_2CT_x, Ti_3CNT_x, and $Ti_3C_2T_x$ MXenes were synthesized using a top-down method.[11,24] First, 0.8 g of LiF (97%, Alfa Aesar) was added to 10 mL of 9 M HCl (prepared from 36 wt % HCl, Alfa Aesar) and stirred for 5 min in a 50 mL plastic centrifuge tube. 0.5 g of a MAX powder was then slowly mixed in the solution. Etching time (temperature) for Ti_2CT_x and $Ti_3C_2T_x$ MXenes were 36 h (35 °C) and for Ti_3CNT_x 18 h (40 °C). After etching, the mixtures were washed with deionized water until the pH of the supernatant reached 6 according to indicator paper. 35 mL of DI water was then added to the mixture followed by a 30 min mild water bath sonication (Bransonic M2800H). MXene colloidal solutions were received by 1h centrifugation of the sonicated suspensions at 3500 rpm (Thermo Fisher Scientific Sorvall ST8 Centrifuge) to separate and remove the precipitated solids. The concentration of each as-prepared MXene solution was ∼5 mg/mL. Between synthesis and start of the measurements, the pH of MXene colloids continued to drop (Table S1) due to diffusion of intercalated acidic species out of the MXene interlayer space. This explains the

https://doi.org/10.1021/acs.inorgchem.2c00537
Inorg. Chem. 2022, 61, 9877−9887

differences between the pH of the supernatant (pH = 6) and blank solutions in Table S1 measured at the onset of experiments. The XRD patterns in Figure S1 confirm successful synthesis and delamination of MXenes. The flake sizes of all synthesized MXenes are similar (~0.8 μm according to AFM (Figure S3)).

Preparation of MXene Samples for Degradation Studies. MXene samples with different pH values for UV−vis, Raman, and XRD measurements were prepared by adding 250 μL of DI water, 1 M HCl, 1 M NaCl, or 1 M NaOH, to 15 mL of MXene solutions in 20 mL glass vials (Wheaton 986560 borosilicate glass vial). The vials were closed and placed in a 70 °C oven to accelerate the reactions.

MXene samples with different pH values for gas collection and GC measurements were prepared by adding 100 μL of DI water, 1 M HCl, 1 M NaCl, or 1 M NaOH, to 6 mL MXene solutions in 10 mL glass vials (Wheaton, screw thread headspace vial, 18 mm diameter). The vials were placed upside down in a 70 °C oven.

Ti_2CT_x samples with different amounts of NaOH added, named Ti_2CT_x-NaOH-1, Ti_2CT_x-NaOH-2, Ti_2CT_x-NaOH-3, and Ti_2CT_x-NaOH-4, were prepared by adding 50, 100, 200, or 800 μL of 1 M NaOH, respectively, to 15 mL MXene solutions in 20 mL glass vials. To bring MXene concentrations in each vial to the same level, 750, 700, 600, or 0 μL of DI water was added to the four samples above, respectively. The vials were closed and placed in a 70 °C oven to accelerate the reactions.

Ti_2CT_x samples for Raman analysis of the gas phase were prepared with a base or antioxidant added to 6 mL MXene solutions in 10 mL glass vials. Sample names and preparation details are listed in Table S2. The vials were closed and placed upside down in a 70 °C oven.

Preparation of MXene Films for Electrical Conductivity Tests. MXene films for conductivity tests were prepared by vacuum filtration of MXene aqueous solutions using 25 mm diameter mixed cellulose ester membranes (Shanghai Bandao Co., 0.45 μm pore size).

Characterization. UV−vis spectra of MXene solutions were recorded over time in a 1 cm optical path quartz cuvette in the range of wavelengths 200−900 nm using a fiber optics QE Pro UV−vis spectrometer (Ocean Optics). Right before sampling, the MXene solution was manually shaken to average its concentration and a 20 μL aliquot was transferred into the quartz cuvette, diluted with 1 mL of DI water, and measured immediately to minimize potential effects of precipitation.

Raman spectra of reacting MXenes over time were recorded after drying a 20 μL aliquot of each MXene solution on a cover glass using a 532 nm laser with 1200 lines/mm grating, 100× objective, 20s exposure time, 0.1% laser power, and 10 accumulations. Raman spectra of the gas phase of MXene samples over time were recorded using a 532 nm laser with 1200 lines/mm grating, 5× objective, 20s exposure time, 100% laser power, and 10 accumulations. All Raman spectra in this work were collected with a Renishaw InVia confocal Raman microspectrometer.

Gas evolved in MXene degradation processes was analyzed with a Thermal Scientific Trace-1300 gas chromatograph equipped with a fused silica capillary column (Carboxen 1006 PLOT, 30 m length, 0.53 mm diameter, 30 μm thickness) and a thermal conductivity detector (TCD). Helium was used as the carrier and reference gas with flow rates of 4 and 4.3 mL/min, respectively, and the He purge gas flow rate was 5 mL/min. TCD detector and filament temperatures were 230 and 280 °C, respectively. The column temperature was initially held at 50 °C for 4 min after injection, followed by heating at 20 °C/min to 100 °C and holding for 5 min. For the measurements, a 0.1 mL gas aliquot was extracted from the headspace of a sealed vial with MXene solution using a 1 mL gastight syringe (Hamilton) and manually injected in the GC instrument.

pH was measured after the solutions were taken out from the oven and cooled down to RT (25 °C) using a Mettler Toledo S30 SevenEasy pH meter equipped with a Fisher Scientific Accumet electrode (Catalog No.13-620-631). The pH meter was calibrated using pH 4.00, 7.00, and 10.01 buffer solutions before the measurements.

Final solid products of fully decomposed MXenes were characterized using powder X-ray diffraction (XRD, PANalytical, Phillips MPD) with Cu Kα radiation (λ = 1.5406 Å) at U = 45 kV and I = 40 mA.

XPS (ESCALAB 250Xi, Thermo Scientific) equipped with an Al Kα source (1486.6 eV) was used for characterization of MXene surface chemistry and oxidation state of M during MXene degradation. The binding energy was calibrated based on the C 1s line (binding energy 284.8 eV). Charge neutralization was applied. No sputtering was used for the measurements.

The electrical conductivity of MXene membranes prepared by vacuum filtration was measured using a four-point probe (VPF-500, Janis Research Co., Inc.) by varying the current from 100 to 1000 μA depending on the sample resistance. Each reported value was averaged from 10 measurements.

Atomic force microscopy (AFM) was performed using a Digital Instruments Nanoscope IIIA under an ambient atmosphere. The AFM images of MXenes were recorded in tapping mode with a silicon tip (App Nano, tip radius < 10 nm).

RESULTS AND DISCUSSION

MXene Degradation at Different pH Values. The initial pH of MXene solutions was adjusted by adding the same amount of HCl or NaOH (250 μL of 1 M solution) to the samples in Table S1. Blank samples were prepared by adding 250 μL of DI water to MXene solution. Many factors need to be taken into consideration to isolate the effects of pH on the rates of chemical reactions. For example, when comparing the samples containing HCl and NaOH to MXene colloids in pure water, the presence of Na^+ (in the NaOH sample) or Cl^- (in the HCl sample) may potentially interfere with the effects of pH. To disentangle this potential interference and compensate for differences in ionic strength (factor influencing colloidal stability and potentially the rate of hydrolysis) between pure water and electrolyte solutions, we prepared samples with equivalent amounts of background electrolyte NaCl. The names of the samples studied in this work and their corresponding initial pH values are listed in Table S1.

For the thinnest and therefore most reactive Ti-based MXene Ti_2CT_x,[24] visual signs of degradation were already evident after ~6 h at 70 °C (Figure 1a) where MXene flakes in the Ti_2CT_x-HCl sample formed a solid mass floating at the top of the solution supported by trapped gas (CH_4) evolved during

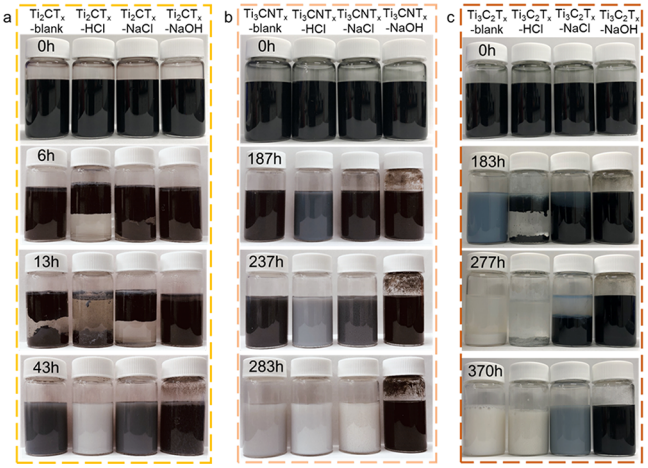

Figure 1. Photographs of MXene aqueous colloids being stored at 70 °C for the indicated times: (a) Ti_2CT_x-blank, Ti_2CT_x-HCl, Ti_2CT_x-NaCl, and Ti_2CT_x-NaOH; (b) Ti_3CNT_x-blank, Ti_3CNT_x-HCl, Ti_3CNT_x-NaCl, and Ti_3CNT_x-NaOH; (c) $Ti_3C_2T_x$-blank, $Ti_3C_2T_x$-HCl, $Ti_3C_2T_x$-NaCl, and $Ti_3C_2T_x$-NaOH.

https://doi.org/10.1021/acs.inorgchem.2c00537
Inorg. Chem. 2022, 61, 9877−9887

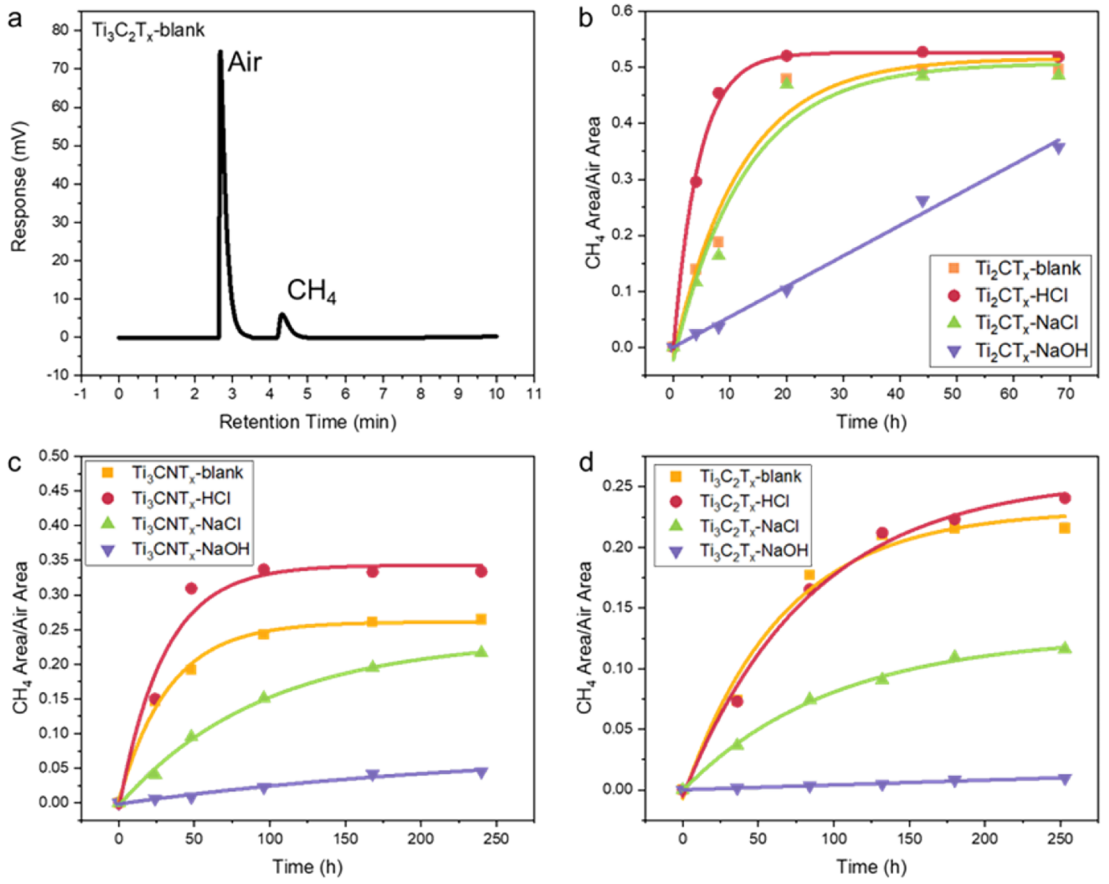

Figure 2. (a) Typical GC elution curve of gaseous products from the $Ti_3C_2T_x$-blank sample. Initial CH_4 evolution kinetics plotted according to GC data at different initial pH values for (b) Ti_2CT_x, (c) Ti_3CNT_x, and (d) $Ti_3C_2T_x$ MXenes (lines are guides to eye).

hydrolysis.[24] Without trapped gas, the agglomerated MXene flakes are expected to precipitate instead of floating. These observations directly indicate fast degradation of the MXene in an acidic environment with relatively rapid gas evolution. Similarly, the MXene in the Ti_2CT_x-blank sample was observed floating on top, albeit after a longer time, ∼13 h. Agglomeration may also happen in the Ti_2CT_x-NaOH sample, but it never formed a floating mass on top, indicating a slower gas evolution (*i.e.*, slower MXene hydrolysis) from this MXene in a basic environment. The amount of gas produced in this sample at any time point was probably too small to support the weight of agglomerated MXene. Visual appearance of Ti_3CNT_x and $Ti_3C_2T_x$ samples (Figure 1b,c) also showed much faster degradation of these MXenes in an HCl-containing environment compared to NaOH, where the solutions retained their homogeneous characteristic dark appearance up until 283 h (Ti_3CNT_x-NaOH) and 370 h ($Ti_3C_2T_x$-NaOH) while all other samples have decomposed into white-colored dispersions (titania).

These visual observations already point to sensitivity of MXene hydrolysis to pH of the environment. However, as mentioned above, more quantitative information on MXene degradation is provided by direct registration of gaseous carbon-containing reaction products with a sensitive GC technique. Using GC, we have shown before that CH_4 is the main gaseous product of carbide MXene degradation in water.[24] CH_4 formation is an unambiguous indicator of MXene degradation as the only way to convert MXene's carbon into a hydrocarbon is to completely break all its bonds to an M element. Here, we monitored CH_4 evolution rates using GC to investigate the degradation kinetics of MXenes at different pH values. Figure 2a shows a typical chromatogram of the head space above the $Ti_3C_2T_x$-blank sample. Since the amount of air in a closed reaction vial is fixed, we used it as the internal standard and the ratio of the area of the chromatographic peak of CH_4 to the area of the air peak as a measure of the CH_4 evolution rate, which is equivalent to the MXene degradation rate. CH_4 evolution rates from the Ti_2CT_x MXene samples follow the order Ti_2CT_x-HCl > Ti_2CT_x-blank ≈ Ti_2CT_x-NaCl > Ti_2CT_x-NaOH (Figure 2b), indicating that at higher pH, CH_4 evolution (MXene degradation) is slower. Interestingly, for Ti_3CNT_x MXene, the CH_4 evolution rate followed the order Ti_3CNT_x-HCl > Ti_3CNT_x-blank > Ti_3CNT_x-NaCl > Ti_3CNT_x-NaOH (Figure 2c), *i.e.*, addition of NaCl, without changing the pH, already suppressed degradation of Ti_3CNT_x MXene. We hypothesize that this may occur because the negatively charged MXene surface attracts Na^+ surrounded by a H_2O hydration shell.[37,38] These Na^+ ions as well as the H_2O molecules in the hydration shell of Na^+ attracted to the MXene surface cannot react with MXene, while at the same time they increase the distance and sterically hinder the approach and reaction of other H_2O molecules from the bulk of water, thus suppressing to some extent MXene hydrolysis. In the case of Ti_2CT_x, we did not observe the slowing-down effect of NaCl, probably because the reactivity of Ti_2CT_x is so much higher compared to the other two thicker MXenes that the steric hindrance has no measurable slowing-down effect on hydrolysis.[24] The CH_4 evolution rate for $Ti_3C_2T_x$ MXene

https://doi.org/10.1021/acs.inorgchem.2c00537
Inorg. Chem. 2022, 61, 9877−9887

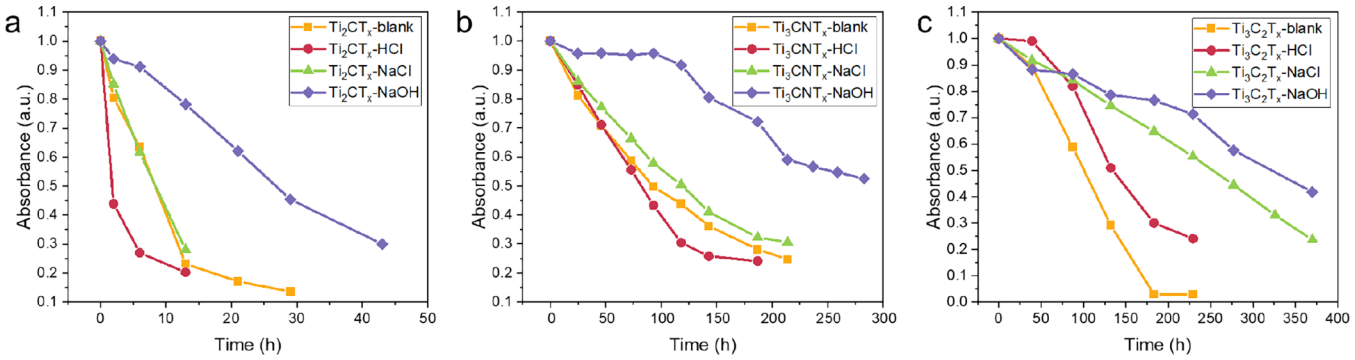

Figure 3. Degradation kinetics of (a) Ti_2CT_x, (b) Ti_3CNT_x, and (c) $Ti_3C_2T_x$ MXenes in aqueous colloids with different electrolytes added. The curves plotted according to UV−vis data.

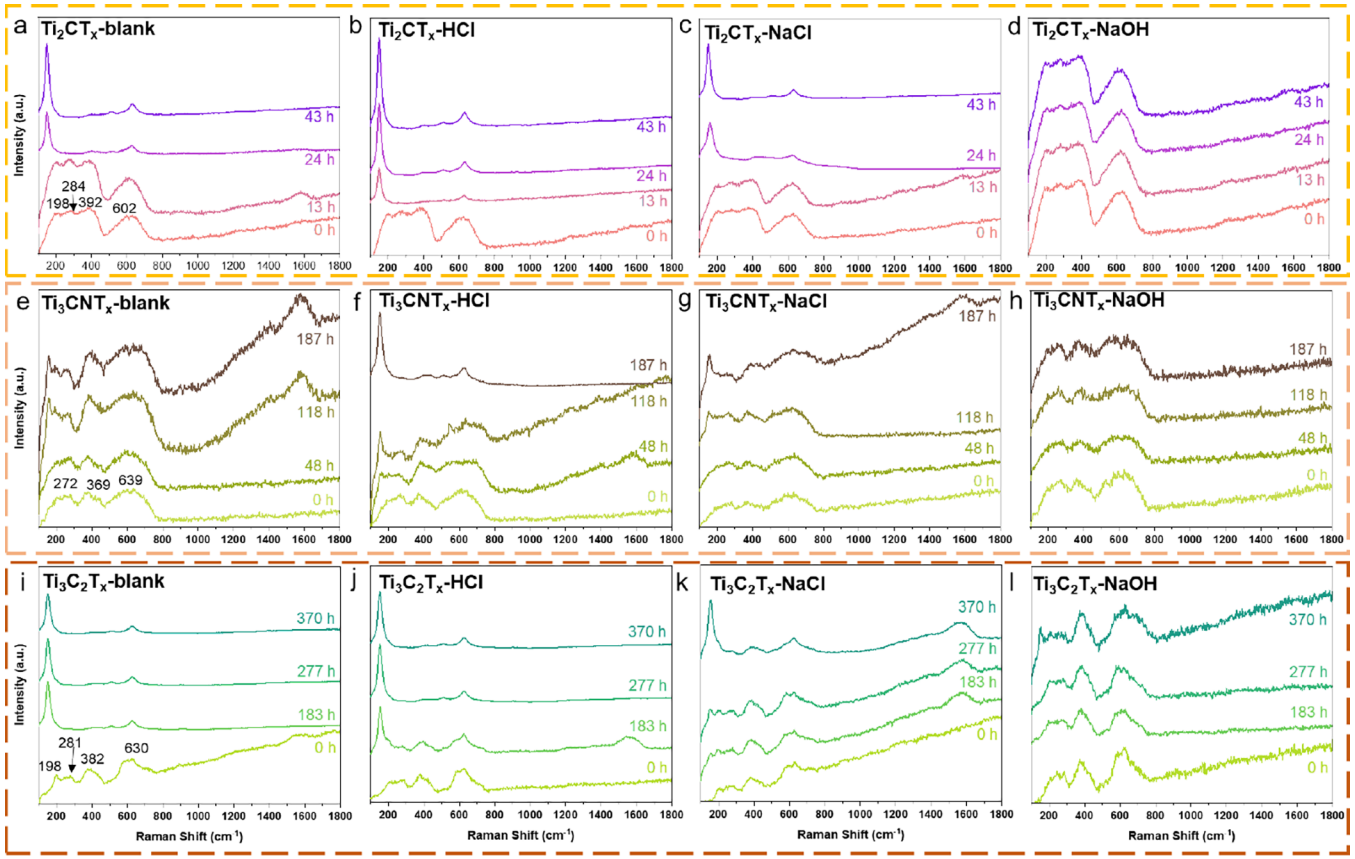

Figure 4. Raman spectra of dry solids collected from (a) Ti_2CT_x-blank, (b) Ti_2CT_x-HCl, (c) Ti_2CT_x-NaCl, (d) Ti_2CT_x-NaOH, (e) Ti_3CNT_x-blank, (f) Ti_3CNT_x-HCl, (g) Ti_3CNT_x-NaCl, (h) Ti_3CNT_x-NaOH, (i) $Ti_3C_2T_x$-blank, (j) $Ti_3C_2T_x$-HCl, (k) $Ti_3C_2T_x$-NaCl, and (l) $Ti_3C_2T_x$-NaOH MXene solutions over time.

followed the order $Ti_3C_2T_x$-HCl ≈ $Ti_3C_2T_x$-blank > $Ti_3C_2T_x$-NaCl > $Ti_3C_2T_x$-NaOH (Figure 2d). Although $Ti_3C_2T_x$-NaOH still showed the slowest degradation rate, the acidic $Ti_3C_2T_x$-HCl degraded more slowly than Ti_2CT_x-HCl and showed a degradation rate similar to $Ti_3C_2T_x$-blank. This can be attributed to a less negative zeta potential of MXene in the presence of H^+,[39] leading to some agglomeration of MXene flakes, which renders them less accessible to hydrolysis (diffusion limitations). On the other hand, although $Ti_3C_2T_x$-blank has a higher pH compared with $Ti_3C_2T_x$-HCl, the flakes in $Ti_3C_2T_x$-blank are well dispersed and more susceptible to hydrolysis. This phenomenon was only observed for the $Ti_3C_2T_x$ sample but not the Ti_2CT_x or Ti_3CNT_x samples, likely because higher reactivities of Ti_2CT_x and Ti_3CNT_x overwhelm the slowing-down effect due to MXene agglomeration.[24]

We support the GC results by monitoring light absorbance of MXene colloids at plasmon resonance maximum over time (Figure 3a−c). For each studied MXene, the value of absorbance at the corresponding plasmon resonance peak maximum was assumed to be proportional to the concentration of the MXene in the solution. This assumption effectively neglects light losses due to scattering, which may not be fully justified, especially in the situation when colloidal stability (particle size) changes between the samples with different pH values and over time of the reaction. Because of this, UV−vis data are inferior to direct registration of gaseous reaction products and are used here as complementary to GC

https://doi.org/10.1021/acs.inorgchem.2c00537
Inorg. Chem. 2022, 61, 9877−9887

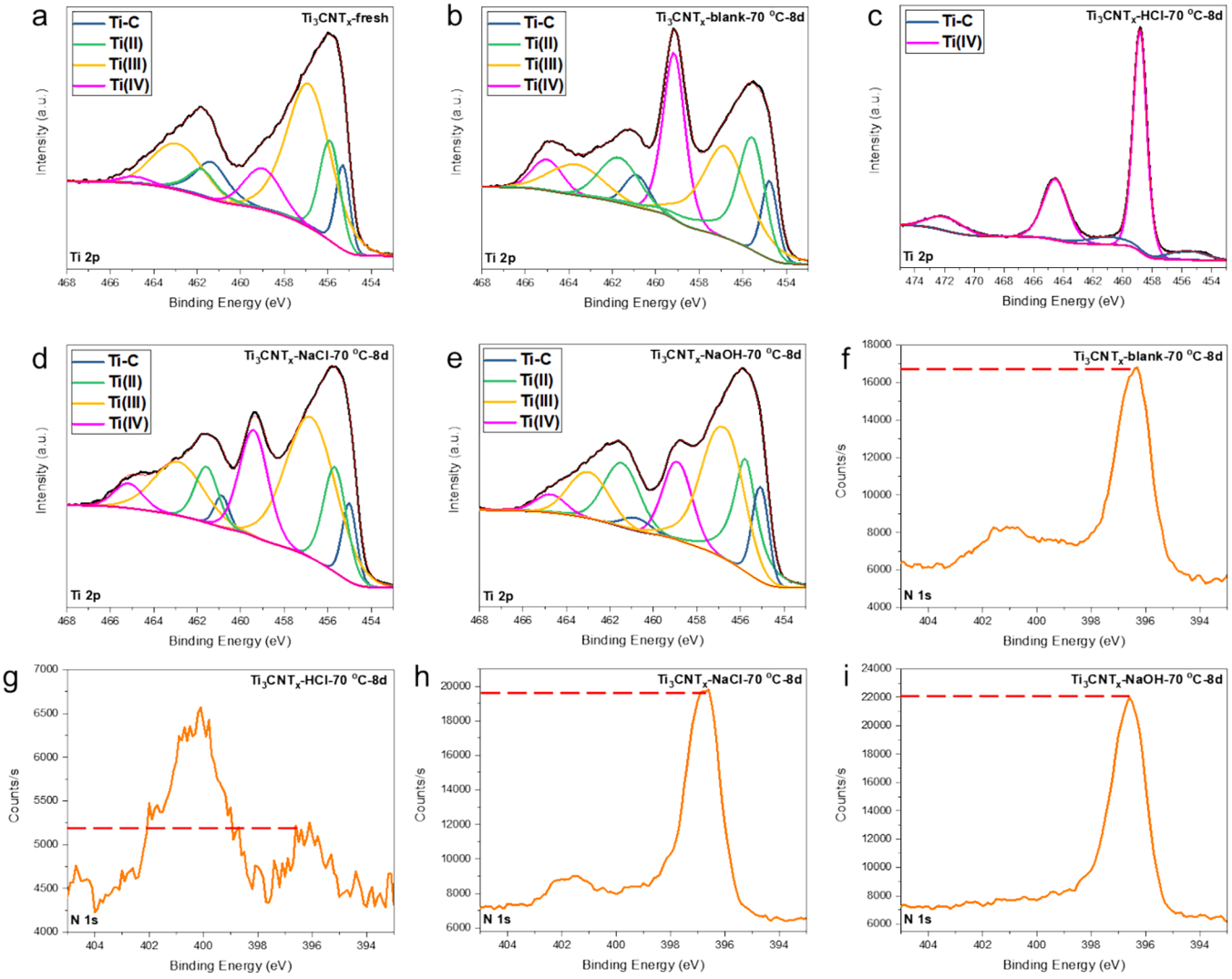

Figure 5. High-resolution XPS spectra of Ti 2p for (a) fresh Ti_3CNT_x, (b) Ti_3CNT_x-blank, (c) Ti_3CNT_x-HCl, (d) Ti_3CNT_x-NaCl, and (e) Ti_3CNT_x-NaOH MXenes after storage at 70 °C for 8 days, and N 1s for (f) Ti_3CNT_x-blank, (g) Ti_3CNT_x-HCl, (h) Ti_3CNT_x-NaCl, and (i) Ti_3CNT_x-NaOH MXenes after storage at 70 °C for 8 days.

data. The UV−vis transmittance spectra of MXenes in different pH environments recorded over time are provided in Figures S4−S6. According to these data, the degradation rates of Ti_2CT_x and Ti_3CNT_x MXene samples follow the same order as the rates obtained from GC results. In addition to Ti_3CNT_x derived from in-house synthesized Ti_3AlCN, repeated experiments with Ti_3CNT_x derived from the commercial Ti_3AlCN MAX phase show the same trend (Figure S7). It seems that the excess of H^+ at acidic pH favors methane formation (according to GC), consuming more carbon faster and accelerating MXene hydrolysis, which is manifested by faster material degradation according to visual observations and UV−vis spectroscopy. The overall degradation rate for $Ti_3C_2T_x$ also decreases with pH in the order similar to the order derived from GC results. However, according to UV−vis, on a short time scale after the start of the experiment, the behavior of this MXene was different: $Ti_3C_2T_x$-NaOH degraded faster within the first 50 h (reproduced in three independent experiments), as evidenced by a rapid drop in absorbance of the solution (Figure 3c). After ∼50 h, the rate of $Ti_3C_2T_x$-NaOH degradation slowed down (reproduced in three independent experiments) and stayed low for the duration of the experiment; thus, the previously observed trend from GC ($Ti_3C_2T_x$-HCl ≈ $Ti_3C_2T_x$-blank > $Ti_3C_2T_x$-NaCl > $Ti_3C_2T_x$-NaOH) was recovered. The experiments with $Ti_3C_2T_x$ samples were repeated at a lower temperature (50 °C, Figure S8) and produced similar results: the degradation of $Ti_3C_2T_x$-NaOH was faster within the first 100 h but then slowed down. This peculiar behavior may be due to a reaction between the −OH groups on the MXene surface with OH^- in the solution producing defected structures that accelerated initial hydrolysis of MXene[36,39] leading to an initially higher degradation rate at basic pH. However, we hypothesize that as the reaction progressed, formation of $Ti(OH)_x$ on the MXene surface protected the flakes from a direct attack by H_2O in the bulk, resulting in a slower degradation after ∼50 h (at 70 °C).

The solids collected over time from MXene solutions degraded at 70 °C (solutions in Figure 1a−c stored) were also analyzed by Raman spectroscopy. These solids at different moments of time since the inception of the experiment represent fresh MXenes, a mix of MXenes with products of their degradation, and finally, the complete degradation products. All spectra of freshly prepared samples (at 0 h) showed typical vibrational modes of the corresponding

https://doi.org/10.1021/acs.inorgchem.2c00537
Inorg. Chem. 2022, 61, 9877−9887

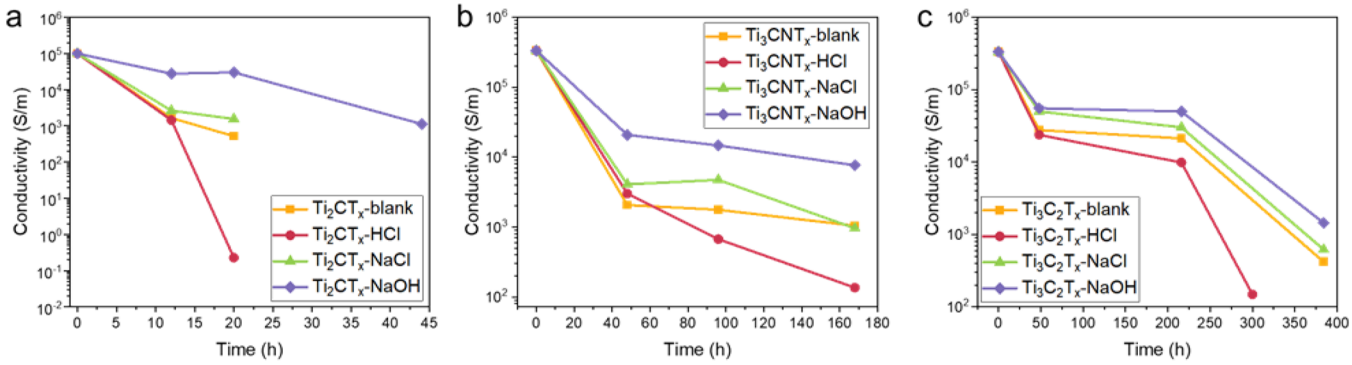

Figure 6. Electrical conductivity of (a) Ti_2CT_x, (b) Ti_3CNT_x, and (c) $Ti_3C_2T_x$ membranes from MXene solutions with different electrolytes over time.

MXenes (Raman shifts at 198, 284, 392, and 602 cm^{-1} for Ti_2CT_x; 272, 369, and 639 cm^{-1} for Ti_3CNT_x; and 198, 281, 382, and 630 cm^{-1} for $Ti_3C_2T_x$).[23,40] A rapid decomposition of the Ti_2CT_x-HCl sample is evidenced by the TiO_2 peak at 150 cm^{-1} appearing after 13 h at 70 °C (Figure 4b), while Ti_2CT_x in other environments largely retained its intact structure at this time point (Figure 4a,c,d). The Ti_2CT_x-blank and Ti_2CT_x-NaCl samples decomposed within 24 h (Figure 4a,c). However, Ti_2CT_x-NaOH still showed the Raman signature of the MXene structure after 43 h treatment at 70 °C (Figure 4d), again demonstrating the superior chemical stability among our Ti_2CT_x samples. These Raman results are in good agreement with GC data (Figure 2) and visual observations (Figure 1a,c) for Ti_2CT_x MXene. Similar conclusions could be drawn from Raman analysis of the solids for Ti_3CNT_x and $Ti_3C_2T_x$ MXenes: while Ti_3CNT_x-HCl, Ti_3CNT_x-blank, and Ti_3CNT_x-NaCl samples were largely decomposed after 187 h (Figure 4e–g), Ti_3CNT_x-NaOH barely started to show the titania peak by that time at all (Figure 4h). Finally, the $Ti_3C_2T_x$-NaOH sample still showed the intact MXene structure with only a small titania peak, even after 370 h at 70 °C (Figure 4l), while $Ti_3C_2T_x$-blank, $Ti_3C_2T_x$-HCl, and $Ti_3C_2T_x$-NaCl have already completely decomposed to titania by that time (Figure 4i–k).

XPS analysis of solids was also performed complementary to GC results on MXene degradation. Figure 5a shows a high-resolution XPS spectrum of Ti 2p for fresh Ti_3CNT_x MXene. The peaks were deconvoluted into Ti-C, Ti(II), Ti(III), and Ti(IV) (Ti in TiO_2) according to published studies.[17,41] Using this procedure with our fresh Ti_3CNT_x sample, the atomic % of Ti(IV) is 9.13%. After 8 days at 70 °C, the atomic % of Ti(IV) grows to 23.33%, 84.44%, 18.45%, and 16.10% for Ti_3CNT_x-blank, Ti_3CNT_x-HCl, Ti_3CNT_x-NaCl, and Ti_3CNT_x-NaOH, respectively (Figure 5b–e), confirming a larger extent of degradation of Ti_3CNT_x MXene in acidic environments compared with less acidic and basic environments. Since degradation of Ti_3CNT_x results in NH_3,[24] a lower intensity of the N 1s peak in the spectrum of solids is expected with a higher extent of degradation. Indeed, as shown in Figure 5f–i, the intensity of the N 1s peak demonstrates the trend: Ti_3CNT_x-NaOH > Ti_3CNT_x-NaCl > Ti_3CNT_x-blank > Ti_3CNT_x-HCl. Overall, the XPS analysis confirms our previous visual observations, GC data, UV–vis, and Raman spectroscopic results, providing solid support for the higher stability of the studied MXenes at higher pH.

Above, we emphasized the necessity and advantages of monitoring direct markers of MXene degradation using well-established techniques of gas analysis, supported by UV–vis spectroscopy and characterization of the solids. Taken together, these data provide a strong support to the conclusion that MXenes dispersed in water are chemically more stable in basic environments compared to acidic environments. An important practical question is how MXene storage in the environments with different pH influences their performance characteristics, for example, electrical conductivity? To investigate this, we have measured electrical conductivity of the MXene films produced from Ti_2CT_x, Ti_3CNT_x, and $Ti_3C_2T_x$ colloidal solutions with different electrolytes over time. Figure 6a shows a rapid drop in conductivity of the Ti_2CT_x-HCl film, in agreement with fast degradation of this MXene in acidic environments. Ti_2CT_x-blank and Ti_2CT_x-NaCl samples are less acidic, and their corresponding films show a slower decrease in conductivity. Ti_2CT_x-HCl, Ti_2CT_x-blank, and Ti_2CT_x-NaCl were completely decomposed before 44 h. However, the Ti_2CT_x-NaOH sample shows the slowest drop due to a higher stability of the MXene in basic environments: the conductivity of this film remains within the measurable range at and after 44 h. Similar considerations apply to Ti_3CNT_x and $Ti_3C_2T_x$ samples (Figure 6b,c), again demonstrating good agreement with slower degradation kinetics observed for these samples according to GC data (Figure 2).

The conductivity of the films prepared from MXene samples drops due to structure degradation. The composition of solid degradation products of the studied MXenes also differs depending on pH. According to XRD patterns, the final degradation products of Ti_2CT_x-blank and Ti_2CT_x-HCl are mixtures of anatase and rutile, while Ti_2CT_x-NaOH and Ti_2CT_x-NaCl have only formed anatase (Figure S9). Similarly, the final degradation products of Ti_3CNT_x and $Ti_3C_2T_x$ are rutile plus anatase in an acidic environment, whereas only anatase was formed in a basic environment (Figure S10). Preferential formation of rutile over anatase in a stronger acidic environment is known in the literature on TiO_2 nanoparticle synthesis.[42]

Effect of Base Concentration on MXene Hydrolysis. The above discussion suggests that a higher pH slows down MXene degradation. Indeed, in experiments with different concentrations of NaOH in the environment (samples Ti_2CT_x-NaOH-1, Ti_2CT_x-NaOH-2, Ti_2CT_x-NaOH-3, and Ti_2CT_x-NaOH-4, where the increasing integers correspond to 50, 100, 200, and 800 μL of 1 M NaOH added), we observed a negative correlation between the concentration of base and the MXene degradation rate (Figure 7a,b, and Figure S11). The Ti_2CT_x-

https://doi.org/10.1021/acs.inorgchem.2c00537
Inorg. Chem. 2022, 61, 9877–9887

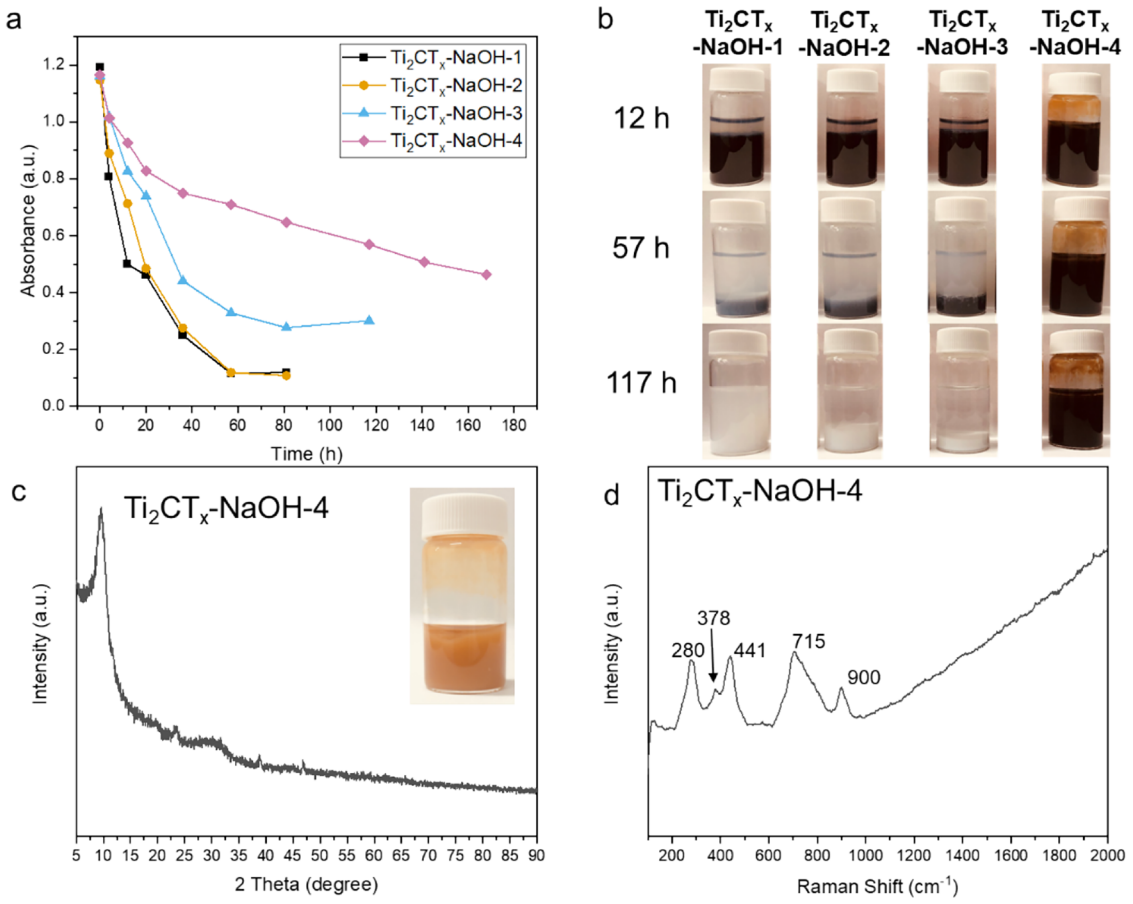

Figure 7. (a) Degradation kinetics (according to UV−vis) and (b) visual appearance over time of Ti_2CT_x MXenes with different concentrations of NaOH added. (c) XRD pattern, optical photograph, and (d) Raman spectrum of the solid residue from Ti_2CT_x-NaOH-4 after complete degradation of the MXene.

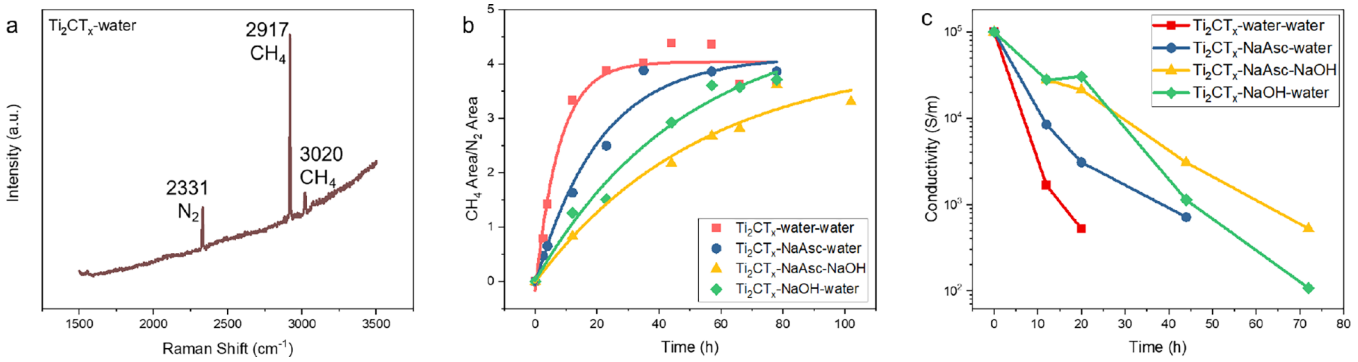

Figure 8. (a) Raman spectrum of the gas phase recorded during degradation of Ti_2CT_x MXene in water in a closed vial. (b) Degradation kinetics of Ti_2CT_x MXene in different aqueous environments. (c) Electrical conductivities of Ti_2CT_x MXene membranes produced by vacuum filtration from different aqueous solutions.

NaOH-4 sample with the highest concentration of NaOH remained basic even after complete degradation of the MXene (final pH = 9, Figure S12). It is worth noting that instead of forming titania, this sample produced layered $Na_2Ti_3O_7$ after complete degradation, according to the XRD pattern (Figure 7c) and Raman spectrum of the solid residue (Figure 7d) where the peaks at 280, 378, 441, 715, and 900 cm^{-1} are characteristic of $Na_2Ti_3O_7$.[43] Similar formation of δ-$M_xV_2O_5{\cdot}nH_2O$ (M = Li, Na, K, Mg, and Ca) was observed before, when V_2CT_x MXene was oxidized in hydrogen peroxide in the presence of alkali metal chlorides.[44] Thus, MXene degradation in aqueous bases can provide an interesting chemical route to layered metalates.

Combination of a Basic Environment and an Antioxidant Suppresses MXene Degradation. Most efforts in the published literature on MXene research were focused on suppressing MXene oxidation. In particular, the use of antioxidants was proposed for this purpose.[31] The importance of direct hydrolysis in MXene degradation processes has been recognized only recently. Therefore, it was interesting to investigate to what extent we can suppress both, hydrolysis and oxidation, the two main chemical

https://doi.org/10.1021/acs.inorgchem.2c00537
Inorg. Chem. 2022, 61, 9877−9887

processes leading to MXene degradation in aqueous colloids. Having figured out that MXenes are hydrolyzed more slowly at a higher pH, we now make the next step and propose that a basic environment combined with the addition of an antioxidant (we used sodium L-ascorbate but potentially other antioxidants can work too) can be a better way to store aqueous MXene colloidal solutions. To check this hypothesis, we prepared different samples with both a base and antioxidant added (Table S2) and monitored CH_4 evolution rates from these samples in closed vials by Raman spectroscopy to determine the kinetics of MXene degradation. Figure 8a shows a typical Raman spectrum of the gas phase recorded during degradation of Ti_2CT_x MXene in water. The peaks at 2917 and 3020 cm^{-1} represent CH_4, and the peak at 2331 cm^{-1} represents N_2. As the N_2 amount in the vial remains fixed, the peak area of CH_4 divided by the area of the N_2 peak gives the relative amount of CH_4 formed during degradation. CH_4 evolution kinetics for different samples are shown in Figure 8b. As expected, the Ti_2CT_x-water-water sample (neither NaOH nor sodium L-ascorbate added) shows the fastest degradation because both hydrolysis and oxidation proceed unsuppressed. Compared with Ti_2CT_x-NaOH-water, the Ti_2CT_x-NaAsc-water sample showed a higher CH_4 evolution rate, *i.e.*, a higher hydrolysis rate (methane is a product of hydrolysis, not oxidation). In accordance with the hypothesis that high pH suppresses hydrolysis and the antioxidant suppresses oxidation of MXenes, a combination of NaOH with NaAsc in Ti_2CT_x-NaAsc-NaOH resulted in the slowest degradation rate and is, therefore, more beneficial for prolonging the shelf life of MXenes. The rate of drop in electrical conductivity of films prepared from these samples followed the order Ti_2CT_x-water−water > Ti_2CT_x-NaAsc-water > Ti_2CT_x-NaOH-water > Ti_2CT_x-NaAsc-NaOH, showing the positive effect of high pH plus antioxidant on a practically important property of MXenes. Since both NaAsc and NaOH are water-soluble, they can be washed out with water, if needed, before using MXenes that were conveniently stored in aqueous colloidal solutions with these additives.

CONCLUSIONS

In summary, the effect of initial pH of aqueous colloidal solution on the degradation of MXenes (Ti_2CT_x, Ti_3CNT_x, and $Ti_3C_2T_x$) has been studied by analysis of evolved gases with GC and Raman spectroscopy, complemented by visual observations, UV−vis spectroscopy, and characterization of solid reaction products with XRD, XPS, and Raman spectroscopy. MXene degradation yields either titania or layered metalates depending on pH. The results of this study show that the degradation of MXenes in aqueous colloidal solutions is suppressed in basic environments specifically due to a reduced rate of MXene hydrolysis. We also propose a combination of a basic environment with the addition of an antioxidant (*e.g.*, sodium ascorbate) as an effective way to suppress both hydrolysis and oxidation of MXenes in aqueous colloidal solutions, thus further prolonging their shelf life compared to when either one of these strategies is employed alone. Both additives are water-soluble and can be easily washed out from MXenes when needed. We believe that these findings are important for further understanding of MXene chemistry, as well as for development of improved storage protocols and applications of MXenes.

ASSOCIATED CONTENT

Supporting Information

The Supporting Information is available free of charge at https://pubs.acs.org/doi/10.1021/acs.inorgchem.2c00537.

XRD patterns of MAX phases and corresponding MXenes; AFM images of Ti_2CT_x, Ti_3CNT_x, and $Ti_3C_2T_x$ MXenes; UV−vis transmittance spectra of MXene aqueous colloids (Ti_2CT_x, Ti_3CNT_x, and $Ti_3C_2T_x$) with different initial pH values stored at 70 °C recorded over time; degradation kinetics of $Ti_3C_2T_x$ MXenes in aqueous colloids with different electrolytes added at 50 °C measured by UV−vis spectroscopy; XRD patterns of final degradation products collected from Ti_2CT_x, Ti_3CNT_x, and $Ti_3C_2T_x$ MXenes with different initial pH values; UV−vis transmittance spectra of Ti_2CT_x with different initial amounts of NaOH added stored at 70 °C recorded over time; time dependence of pH of Ti_2CT_x MXene aqueous colloids with different initial amounts of NaOH added; initial pH values of MXene samples prepared for UV−vis analysis; description of MXene samples prepared for gas phase analysis (PDF)

AUTHOR INFORMATION

Corresponding Author

Vadym N. Mochalin − *Department of Chemistry, Missouri University of Science & Technology, Rolla, Missouri 65409, United States; Department of Materials Science & Engineering, Missouri University of Science & Technology, Rolla, Missouri 65409, United States;* orcid.org/0000-0001-7403-1043; Email: mochalinv@mst.edu

Author

Shuohan Huang − *State Key Laboratory for Modification of Chemical Fibers and Polymer Materials, College of Materials Science and Engineering, Donghua University, Shanghai 201620, China; Department of Chemistry, Missouri University of Science & Technology, Rolla, Missouri 65409, United States;* orcid.org/0000-0002-8800-5249

Complete contact information is available at: https://pubs.acs.org/10.1021/acs.inorgchem.2c00537

Notes

The authors declare no competing financial interest.

ACKNOWLEDGMENTS

The authors thank Jiancheng Wang (DHU), Lei Zhu (DHU), and Prof. Yumin Xia (DHU) for help with XPS measurements, Justin Nulsen (Missouri S&T) for help with MAX phase synthesis, and Material Research Center (Missouri S&T) for providing access to X-ray diffractometer. This work was partially supported by the National Science Foundation under Grant No. MoMS 1930881. This work was also supported by the Fundamental Research Funds for the Central Universities 2232022D-03.

REFERENCES

(1) Iqbal, A.; Shahzad, F.; Hantanasirisakul, K.; Kim, M.-K.; Kwon, J.; Hong, J.; Kim, H.; Kim, D.; Gogotsi, Y.; Koo, C. M. Anomalous absorption of electromagnetic waves by 2D transition metal carbonitride Ti_3CNT_x (MXene). *Science* **2020**, *369*, 446−450.

(2) Huang, S.; Mutyala, K. C.; Sumant, A. V.; Mochalin, V. N. Achieving superlubricity with 2D transition metal carbides (MXenes) and MXene/graphene coatings. *Mater. Today Adv.* **2021**, *9*, 100133.
(3) Guo, Y.; Zhong, M.; Fang, Z.; Wan, P.; Yu, G. A wearable transient pressure sensor made with MXene nanosheets for sensitive broad-range human-machine interfacing. *Nano Lett.* **2019**, *19*, 1143−1150.
(4) Abdolhosseinzadeh, S.; Jiang, X.; Zhang, H.; Qiu, J.; Zhang, C. J. Perspectives on solution processing of two-dimensional MXenes. *Mater. Today* **2021**, *48*, 214−240.
(5) Lipatov, A.; Lu, H.; Alhabeb, M.; Anasori, B.; Gruverman, A.; Gogotsi, Y.; Sinitskii, A. Elastic properties of 2D $Ti_3C_2T_x$ MXene monolayers and bilayers. *Sci. Adv.* **2018**, *4*, No. eaat0491.
(6) Ghidiu, M.; Lukatskaya, M. R.; Zhao, M. Q.; Gogotsi, Y.; Barsoum, M. W. Conductive two-dimensional titanium carbide 'clay' with high volumetric capacitance. *Nature* **2014**, *516*, 78−81.
(7) Maleski, K.; Shuck, C. E.; Fafarman, A. T.; Gogotsi, Y. The broad chromatic range of two-dimensional transition metal carbides. *Adv. Opt. Mater.* **2020**, *9*, 2001563.
(8) Borysiuk, V.; Mochalin, V. N. Thermal stability of two-dimensional titanium carbides $Ti_{n+1}C_n$ (MXenes) from classical molecular dynamics simulations. *MRS Commun.* **2019**, *9*, 203−208.
(9) Deysher, G.; Shuck, C. E.; Hantanasirisakul, K.; Frey, N. C.; Foucher, A. C.; Maleski, K.; Sarycheva, A.; Shenoy, V. B.; Stach, E. A.; Anasori, B. Synthesis of Mo_4VAlC_4 MAX phase and two-dimensional Mo_4VC_4 MXene with five atomic layers of transition metals. *ACS Nano* **2019**, *14*, 204−217.
(10) Naguib, M.; Mashtalir, O.; Carle, J.; Presser, V.; Lu, J.; Hultman, L.; Gogotsi, Y.; Barsoum, M. W. Two-Dimensional Transition Metal Carbides. *ACS Nano* **2012**, *6*, 1322−1331.
(11) Alhabeb, M.; Maleski, K.; Anasori, B.; Lelyukh, P.; Clark, L.; Sin, S.; Gogotsi, Y. Guidelines for synthesis and processing of two-dimensional titanium carbide ($Ti_3C_2T_x$ MXene). *Chem. Mater.* **2017**, *29*, 7633−7644.
(12) Mashtalir, O.; Naguib, M.; Mochalin, V. N.; Dall'Agnese, Y.; Heon, M.; Barsoum, M. W.; Gogotsi, Y. Intercalation and delamination of layered carbides and carbonitrides. *Nat. Commun.* **2013**, *4*, 1−7.
(13) Dong, Y.; Mallineni, S. S. K.; Maleski, K.; Behlow, H.; Mochalin, V. N.; Rao, A. M.; Gogotsi, Y.; Podila, R. Metallic MXenes: A new family of materials for flexible triboelectric nanogenerators. *Nano Energy* **2018**, *44*, 103−110.
(14) Li, K.; Wang, X.; Li, S.; Urbankowski, P.; Li, J.; Xu, Y.; Gogotsi, Y. An ultrafast conducting polymer@MXene positive electrode with high volumetric capacitance for advanced asymmetric supercapacitors. *Small* **2020**, *16*, 1906851.
(15) Zhang, C. J.; McKeon, L.; Kremer, M. P.; Park, S.-H.; Ronan, O.; Seral-Ascaso, A.; Barwich, S.; Coileáin, C. Ó.; McEvoy, N.; Nerl, H. C.; Anasori, B.; Coleman, J. N.; Gogotsi, Y.; Nicolosi, V. Additive-free MXene inks and direct printing of micro-supercapacitors. *Nat. Commun.* **2019**, *10*, 1795.
(16) Anasori, B.; Lukatskaya, M. R.; Gogotsi, Y. 2D metal carbides and nitrides (MXenes) for energy storage. *Nat. Rev. Mater.* **2017**, *2*, 16098.
(17) Li, G.; Amer, N.; Hafez, H.; Huang, S.; Turchinovich, D.; Mochalin, V. N.; Hegmann, F. A.; Titova, L. V. Dynamical control over terahertz electromagnetic interference shielding with 2D $Ti_3C_2T_y$ MXene by ultrafast optical pulses. *Nano Lett.* **2019**, *20*, 636−643.
(18) Pandey, R. P.; Rasool, K.; Abdul Rasheed, P.; Mahmoud, K. A. Reductive sequestration of toxic bromate from drinking water using lamellar two-dimensional $Ti_3C_2T_x$ (MXene). *ACS Sustainable Chem. Eng.* **2018**, *6*, 7910−7917.
(19) Ihsanullah, I. MXenes (two-dimensional metal carbides) as emerging nanomaterials for water purification. *Chem. Eng. J.* **2020**, *388*, 124340.
(20) Chertopalov, S.; Mochalin, V. N. Environment sensitive photoresponse of spontaneously partially oxidized $Ti_3C_2T_x$ MXene thin films. *ACS Nano* **2018**, *12*, 6109−6116.
(21) Kim, S. J.; Koh, H.-J.; Ren, C. E.; Kwon, O.; Maleski, K.; Cho, S.-Y.; Anasori, B.; Kim, C.-K.; Choi, Y.-K.; Kim, J.; Gogotsi, Y.; Jung, H. T. Metallic $Ti_3C_2T_x$ MXene gas sensors with ultrahigh signal-to-noise ratio. *ACS Nano* **2018**, *12*, 986−993.
(22) Lee, E.; VahidMohammadi, A.; Prorok, B. C.; Yoon, Y. S.; Beidaghi, M.; Kim, D.-J. Room temperature gas sensing of two-dimensional titanium carbide (MXene). *ACS Appl. Mater. Interfaces* **2017**, *9*, 37184−37190.
(23) Huang, S.; Mochalin, V. N. Hydrolysis of 2D transition-metal carbides (MXenes) in colloidal solutions. *Inorg. Chem.* **2019**, *58*, 1958−1966.
(24) Huang, S.; Mochalin, V. N. Understanding chemistry of two-dimensional transition metal carbides and carbonitrides (MXenes) with gas analysis. *ACS Nano* **2020**, *14*, 10251−10257.
(25) Philipp, W. H. *Chemical reactions of carbides, nitrides, and diborides of titanium and zirconium and chemical bonding in these compounds*; NASA Lewis Research Center: Washington, 1966; pp. 1−20.
(26) Remy, H., *Treatise on Inorganic Chemistry*. 11th ed.; Elsevier Pub. Co.: Amsterdam, 1956; Vol. *1*.
(27) Avgustinik, A. I.; Drozdetskaya, G. V.; Ordan'yan, S. S. Reaction of titanium carbide with water. *Powder Metall. Met. Ceram.* **1967**, *6*, 470−473.
(28) Zhang, C. J.; Pinilla, S.; McEvoy, N.; Cullen, C. P.; Anasori, B.; Long, E.; Park, S.-H.; Seral-Ascaso, A.; Shmeliov, A.; Krishnan, D.; Morant, C.; Liu, X.; Duesberg, G. S.; Gogotsi, Y.; Nicolosi, V. Oxidation stability of colloidal 2D titanium carbides (MXenes). *Chem. Mater.* **2017**, *29*, 4848−4856.
(29) Chae, Y.; Kim, S. J.; Cho, S.-Y.; Choi, J.; Maleski, K.; Lee, B.-J.; Jung, H.-T.; Gogotsi, Y.; Lee, Y.; Ahn, C. W. An investigation into the factors governing the oxidation of two-dimensional Ti_3C_2 MXene. *Nanoscale* **2019**, *11*, 8387−8393.
(30) Zhang, J.; Kong, N.; Hegh, D.; Usman, K. A. S.; Guan, G.; Qin, S.; Jurewicz, I.; Yang, W.; Razal, J. M. Freezing titanium carbide aqueous dispersions for ultra-long-term storage. *ACS Appl. Mater. Interfaces* **2020**, *12*, 34032−34040.
(31) Zhao, X.; Vashisth, A.; Prehn, E.; Sun, W.; Shah, S. A.; Habib, T.; Chen, Y.; Tan, Z.; Lutkenhaus, J. L.; Radovic, M.; Green, M. J. Antioxidants unlock shelf-stable $Ti_3C_2T_x$ (MXene) nanosheet dispersions. *Matter* **2019**, *1*, 513−526.
(32) Xia, F.; Lao, J.; Yu, R.; Sang, X.; Luo, J.; Li, Y.; Wu, J. Ambient oxidation of Ti_3C_2 MXene initialized by atomic defects. *Nanoscale* **2019**, *11*, 23330−23337.
(33) Natu, V.; Hart, J. L.; Sokol, M.; Chiang, H.; Taheri, M. L.; Barsoum, M. W. Edge capping of 2D-MXene sheets with polyanionic salts to mitigate oxidation in aqueous colloidal suspensions. *Angew. Chem., Int. Ed.* **2019**, *58*, 12655−12660.
(34) Shuck, C. E.; Han, M.; Maleski, K.; Hantanasirisakul, K.; Kim, S. J.; Choi, J.; Reil, W. E. B.; Gogotsi, Y. Effect of Ti_3AlC_2 MAX phase on structure and properties of resultant $Ti_3C_2T_x$ MXene. *ACS Appl. Nano Mater.* **2019**, *2*, 3368−3376.
(35) Mathis, T. S.; Maleski, K.; Goad, A.; Sarycheva, A.; Anayee, M.; Foucher, A. C.; Hantanasirisakul, K.; Shuck, C. E.; Stach, E. A.; Gogotsi, Y. Modified MAX phase synthesis for environmentally stable and highly conductive Ti_3C_2 MXene. *ACS Nano* **2021**, *15*, 6420−6429.
(36) Zhao, X.; Vashisth, A.; Blivin, J. W.; Tan, Z.; Holta, D. E.; Kotasthane, V.; Shah, S. A.; Habib, T.; Liu, S.; Lutkenhaus, J. L.; Radovic, M.; Green, M. J. pH, nanosheet concentration, and antioxidant affect the oxidation of $Ti_3C_2T_x$ and Ti_2CT_x MXene dispersions. *Adv. Mater. Interfaces* **2020**, *7*, 2000845.
(37) Doo, S.; Chae, A.; Kim, D.; Oh, T.; Ko, T. Y.; Kim, S. J.; Koh, D.-Y.; Koo, C. M. Mechanism and kinetics of oxidation reaction of aqueous $Ti_3C_2T_x$ suspensions at different pHs and temperatures. *ACS Appl. Mater. Interfaces* **2021**, *13*, 22855−22865.
(38) Ghidiu, M.; Halim, J.; Kota, S.; Bish, D.; Gogotsi, Y.; Barsoum, M. W. Ion-exchange and cation solvation reactions in Ti_3C_2 MXene. *Chem. Mater.* **2016**, *28*, 3507−3514.

https://doi.org/10.1021/acs.inorgchem.2c00537
Inorg. Chem. 2022, 61, 9877−9887

(39) Natu, V.; Sokol, M.; Verger, L.; Barsoum, M. W. Effect of edge charges on stability and aggregation of $Ti_3C_2T_z$ MXene colloidal suspensions. *J. Phys. Chem. C* **2018**, *122*, 27745−27753.
(40) Sarycheva, A.; Gogotsi, Y. Raman spectroscopy analysis of the structure and surface chemistry of $Ti_3C_2T_x$ MXene. *Chem. Mater.* **2020**, *32*, 3480−3488.
(41) Natu, V.; Benchakar, M.; Canaff, C.; Habrioux, A.; Celerier, S.; Barsoum, M. W. A critical analysis of the X-ray photoelectron spectra of $Ti_3C_2T_z$ MXenes. *Matter* **2021**, 1224.
(42) Tsega, M.; Dejene, F. B. Influence of acidic pH on the formulation of TiO_2 nanocrystalline powders with enhanced photoluminescence property. *Heliyon* **2017**, *3*, No. e00246.
(43) Zhang, Z.; Goodall, J. B. M.; Brown, S.; Karlsson, L.; Clark, R. J. H.; Hutchison, J. L.; Rehman, I. U.; Darr, J. A. Continuous hydrothermal synthesis of extensive 2D sodium titanate ($Na_2Ti_3O_7$) nano-sheets. *Dalton Trans.* **2010**, *39*, 711−714.
(44) Ridley, P.; Gallano, C.; Andris, R.; Shuck, C. E.; Gogotsi, Y.; Pomerantseva, E. MXene-Derived Bilayered Vanadium Oxides with Enhanced Stability in Li-Ion Batteries. *ACS Appl. Energy Mater.* **2020**, *3*, 10892−10901.

https://doi.org/10.1021/acs.inorgchem.2c00537
Inorg. Chem. 2022, 61, 9877−9887